Biophysical Journal Volume 99 December 2010 3657–3665

Self-Association of Models of Transmembrane Domains of ErbB Receptors in a Lipid Bilayer

Anupam Prakash, Lorant Janosi, and Manolis Doxastakis*
Department of Chemical and Biomolecular Engineering, University of Houston, Houston, Texas

ABSTRACT Association of transmembrane (TM) helices is facilitated by the close packing of small residues present along the amino-acid sequence. Extensive studies have established the role of such small residue motifs (GxxxG) in the dimerization of Glycophorin A (GpA) and helped to elucidate the association of TM domains in the epidermal growth factor family of receptors (ErbBs). Although membrane-mediated interactions are known to contribute under certain conditions to the dimerization of proteins, their effect is often considered nonspecific, and any potential dependence on protein sequence has not been thoroughly investigated. We recently reported that the association of GpA is significantly assisted by membrane-induced contributions as quantified in different lipid bilayers. Herein we extend our studies to explore the origin of these effects and quantify their magnitude using different amino-acid sequences in the same lipid environment. Using a coarse-grained model that accounts for amino-acid specificity, we perform extensive parallel Monte Carlo simulations of ErbB homodimerization in dipalmitoyl-phosphatidylcholine lipid bilayers. A detailed characterization of dimer formation and estimates of the free energy of association reveal that the TM domains show a significant affinity to self-associate in lipid bilayers, in qualitative agreement with experimental findings. The presence of GxxxG motifs enhances favorable protein-protein interactions at short separations. However, the lipid-induced attraction presents a more complex character than anticipated. Depending on the interfacial residues, lipid-entropic contributions support a decrease of separation or a parallel orientation to the membrane normal, with important implications for protein function.

INTRODUCTION

Transmembrane (TM) proteins are key to numerous biochemical and biophysical processes in living organisms. Several factors contribute to the assembly of individual helical TM proteins into an overall functional structure (1–3). Direct protein-protein interactions play a prominent role, as quantified with the use of amino-acid mutations; however, lipid-mediated effects can add significant contributions that are challenging to discern in such studies. For nonspecific association, both theory and simulations predict that the fluid membrane environment is sufficient to induce association due to perturbations imposed by the proteins at short and intermediate length scales (4–7). It is unclear how such effects would scale for models that include a description of the amino-acid sequence.

Protein association often displays significant specificity, and TM domains form well-defined interfaces along their sequences. In certain cases, this interface is defined by specific motifs, such as the GxxxG motif between small glycine residues, without any strong polar interactions. Dimerization of Glycophorin A (GpA) is considered a prototype of such specificity and has been studied extensively for more than a decade (8–12). Stabilization of the dimer is assisted by small residue sizes, which enhance packing and maximize the area of the interface between the helices. The latter is considered a measure of protein-protein interactions. Furthermore, the lack of side-chain atoms in glycine residues reduces potential unfavorable entropic contributions resulting from a restriction of rotational modes (8). Despite these plausible mechanisms, however, there are still several features that remain unclear. Doura and Fleming (13) showed that mutations that abolish the motif can lead to sequences that still dimerize. Even more surprising was their finding that residues distant from the interface modulate the dimerization affinity, potentially due to structural rearrangements. In a recent study using implicit membrane models, Zhang and Lazaridis (14) supported the notion that residues outside the interface can play a role in accessing GxxxG motifs.

Quantifying lipid-induced contributions in systems that demonstrate sequence-specific association remains a formidable challenge for both simulation and experimental studies. MacKenzie et al. (11) suggested that because of the similarity between lipid-protein and protein-protein enthalpic interactions, specificity is not promoted by the environment. In contrast, Johnson et al. (15) reported that lipid-protein enthalpic interactions do contribute to dimer stability, and quantified the extent of such interactions by estimating the lipid-accessible surface area of the dimer. Entropic contributions can also be important for both proteins (16) and lipids. However, as noted above, changes in lipid entropic contributions are commonly studied by means of simulations lacking amino-acid detail (4–7). Protein tilting and rotational modes present characteristic times that range from 0.1 to 100 μs (17–19) for single TM domains, to even longer times for oligomers. These slow rotational modes impose severe limitations on studies

Submitted July 5, 2010, and accepted for publication October 15, 2010.
*Correspondence: edoxastakis@uh.edu
Editor: Huey W. Huang.

0006-3495/10/12/3657/9 $2.00
doi: 10.1016/j.bpj.2010.10.023

attempting to probe the sequence-specific association of helices by atomistic (AT) simulations. The development of coarse-grained (CG) models that retain a level of amino-acid specificity (20,21) has significantly facilitated the study of TM protein association in lipid bilayers, as in a recent work that examined the effect of mutations on GpA dimerization (22).

Our group focuses on developing parallel Monte Carlo methods that can enable drastic conformational sampling of all degrees of freedom and provide the potential of mean force (PMF) or free energy as a function of separation (23,24). In a previous study using CG models, we examined GpA association and found excellent agreement between our predictions and experimental data on structural and thermodynamic properties (24). Furthermore, detailed insight into the differences observed in three distinct lipid environments suggested that although sequence-specificity was always observed, membrane thickness and rigidity modulate the accessible interfaces. By decomposing the free-energy profile, we calculated a significant lipid-induced attraction at short separations that depends on lipid chemistry.

In this study, we examined the dimerization of helices from a different view, by quantifying association in the same lipid environment using substantially different amino-acid sequences. We selected as model systems the four TM domains of the family of epidermal growth factor receptors (ErbBs). Our choice was driven by the critical role played by these TM proteins in signal transduction mechanisms (25–27). We emphasize, though, that our aim was to probe self-association and not activity. Several studies have indicated that dimerization is a necessary but not sufficient condition for activation (28–30). Nevertheless, contributions from TM domains are important (31–36), and preventing association may inhibit activity (37–39). Although various studies have examined the association thermodynamics of ErbBs by experiment (18,36,40–42), to the best of our knowledge, molecular modeling has not been employed to obtain such predictions in lipid membranes.

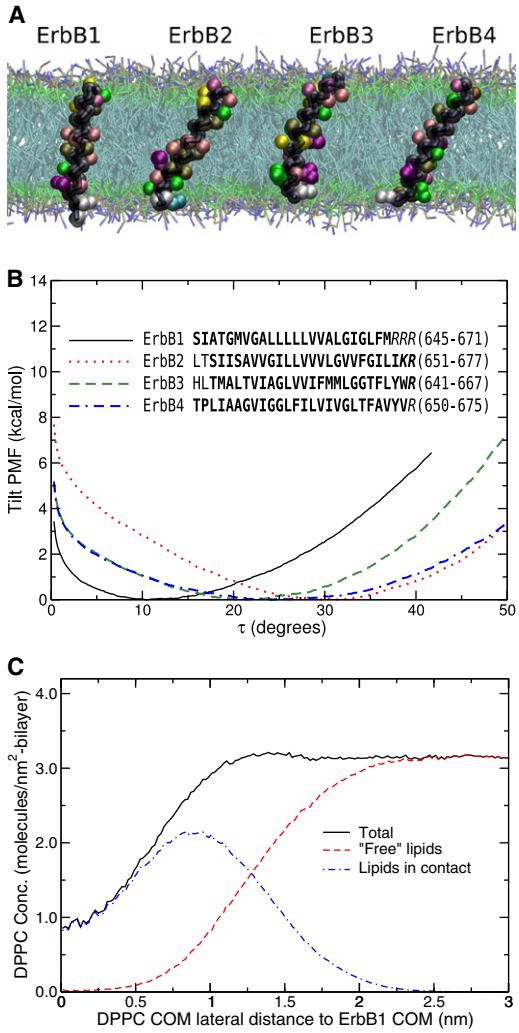

FIGURE 1 (*A*) Models of the TM domains studied. (*B*) The free-energy change as a function of tilt angle τ for each TM sequence studied (27 amino acids, helical domains are in bold; charged residues are in italic). (*C*) ErbB1 COM-to-DPPC COM lateral radial distribution function, with decomposition to lipid molecules in the first layer.

MATERIALS AND METHODS

A sequence of 27 amino acids was selected for each ErbB TM domain model described by the CG MARTINI force field (20). As is common with such models, the secondary structure was maintained through specific potential terms. Using a hierarchical approach, we first performed fully AT simulations with single TM domains of 35 residues in di-palmitoyl phosphatidylcholine (DPPC) bilayers. We employed the GROMOS 53a6 force field and sampled trajectories for 60 ns using standard molecular-dynamics methods (43–45) at 323 K, as in our previous work with GpA (23). The conformational analysis, hydrogen-bonding network, and residue distribution along the membrane normal provided support for a TM helical domain of 23–26 amino acids along the sequence of each protein. Details of the sequences and the extent of the helical domains are provided in the legend of Fig. 1 *B*.

To further characterize these TM domains, we calculated the free-energy change as a function of tilt angle τ (23,46) with the CG model, and measured their surface areas and volumes with both the AT and CG models. The average tilt of ErbB TM domains can be ranked in decreasing order as ErbB2 (~31 °) > ErbB4 (~24 °) > ErbB3 (~21°) > ErbB1 (~10°). We attribute the low tilt angle of ErbB1 to the presence of successive arginine residues at the C-terminus. The actual value is in agreement with experiment data (47). ErbB2 exhibits the highest tilt angle, and the model predicts that ErbB4 is the TM domain that samples the widest span of τ. We calculated the areas and volumes using the g_sas tool provided by GROMACS (45), modified to account for the size of the CG beads. The algorithm is based on the method of Eisenhaber et al. (48), which provides the solvent-accessible surface area (SASA) and solvent-excluded volume (SEV) augmented by the probe radius (49,50). In the first four columns of Table 1 we compare the areas and volumes of single helices using a probe radius of 0.14 nm. This is a typical value for simulations corresponding to water as a solvent, which is not necessarily the most appropriate herein, as discussed further in the Results section. Calculations are shown for both CG models and AT representations. Although the areas appear to be in good agreement, the volumes are overestimated by the CG model. Given the small size of the probe relative to the CG bead size (diameter 0.43–0.47 nm), it is not surprising to find deviations. However, both descriptions agree that ErbB3 is the largest helix in terms of area and volume. Such an estimate is in agreement with ErbB3

TABLE 1 SASA (in nm^2) and SEV (in nm^3) from AT and CG simulations

	A_{Single} CG	A_{Single} AT	V_{Single} CG	V_{Single} AT	A_{Interf} CG
ErbB1	27.4	27.5	5.83	5.33	12.7
ErbB2	27.1	26.4	5.86	5.25	10.5
ErbB3	28.9	28.8	6.41	5.70	12.1
ErbB4	26.8	26.5	5.81	5.14	11.7

exhibiting a single GxxxG motif, in contrast to the other members of the family, which present two such sequences (36).

We studied the self-association of ErbB TM domains by performing (MW)^2-XDOS Monte Carlo simulations in DPPC at 323 K (23,24). This method relies on the expanded ensemble density of states algorithm (51–53), with several critical improvements that include a new parallelization scheme and efficient preferential sampling in the proximity of the proteins (23). All four systems studied included two proteins, 512 lipids, 6000 water molecules, and necessary counterions. A total of 128 unconstrained walkers were used for each TM domain (total of 512) with lateral separation of the centers of mass (COMs, ξ) up to 5.4 nm (4.6 nm for ErbB1). While this manuscript was under review, estimates of the GpA dimerization affinity with the MARTINI force field were reported in a study using umbrella-sampling molecular-dynamics simulations with structures derived by pulling from the dimerized state up to 2.5 nm (54). Despite agreement with our earlier work regarding the significance of lipid-induced attraction, the free energies extracted are somewhat lower than our previous estimates (24). We note that in our method, any pair (out of hundreds) is able to experience large separations where no correlations persist. As discussed in our previous work (24), the minimum interhelical distance can be substantially lower than the lateral COM separation (due to tilting with contacts formed occasionally even when the COMs are 2–3 nm apart). In addition, membrane-induced correlations persist to even longer distances, and herein we expand on this feature. We define a lipid molecule as being in contact when any of the lipid CG beads are within 0.5 nm of any protein bead. Fig. 1 *C* presents the lateral protein COM-to-lipid COM radial distribution function with explicit contributions from proximal lipids. Integration along cylindrical coordinates yields a value of $\approx$15 lipids in contact, which, not surprisingly, is higher than the number of experimentally determined motional restricted lipids (6–12) for α-helices (55) (our calculation accounts only for proximity, and not for dynamics). However, it is important to note that the first lipid solvation shell reaches up to $\approx$2nm; for all other sequences, higher tilting extends this layer to longer distances. Therefore, to fully account for positive contributions corresponding to desolvation of lipids (opposing favorable protein-protein attraction), and to probe uncorrelated structures, the helices must experience lateral COM separations beyond 4 nm.

Finally, although we provided several technical details in previous work (23,24), we should add here that in all of our simulations, convergence was satisfied by low values of the weights modification factor recovering detailed balance and limiting further changes ($\ln f < 10^{-8}$). Apart from the PMF calculation by weights, the free energy can be extracted by projected forces at each ξ-value. Approximately 2×10^5 force values were stored at each bin, sampled every 2.5×10^5 MC steps (using a mix of MC moves (24)) at late stages when $\ln f < 10^{-6}$. Errors on mean forces were calculated by block-averaging (50 values) with PMF errors estimated by subsequent bootstrapping with randomly sampled forces up to 2 standard deviations at each ξ (56,57). Representative accumulated forces with corresponding errors on these mean values are shown in Fig. 2 for ErbB1 and ErbB4.

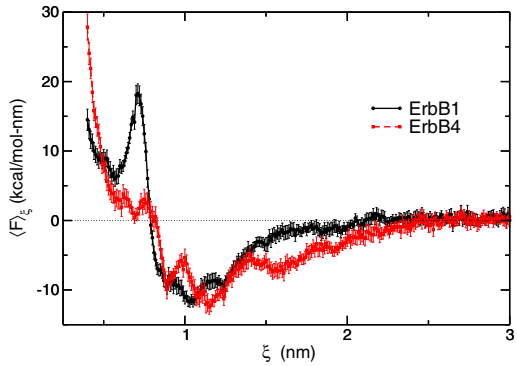

FIGURE 2 Mean projected forces along ξ and estimates of errors (95% confidence intervals) extracted by block averaging for ErbB1 and ErbB4 at close separation.

RESULTS

PMF

The extracted PMF as a function of ξ is presented in Fig. 3 for all systems studied, together with a decomposition into separate contributions (ion contributions were negligible and were omitted for clarity). Dimerization is favorable for all four TM domains, consistent with experimental studies (36,40,42). The strongest association is found for ErbB4, and the weakest is found for ErbB1. The variation in predicted dimerization affinities is greater compared to our previous findings from GpA in three lipid bilayer systems (24), although several common features are recognized. Wide minima are prominent for helices that tilt extensively, due to differences in the ability of the reaction coordinate (lateral separation) to probe changes along the interface of the dimer (24). A first look at the decomposed profiles reveals that ErbB1 helices, in contrast to the other TM domains (and GpA in our previous work), remain at distances where protein-protein contributions are close to their minimum. We will analyze this feature further below. The PMF minimum for ErbB3 is at $\approx$1 nm, whereas for the other members it is at $\approx$0.8 nm. For all of the proteins,

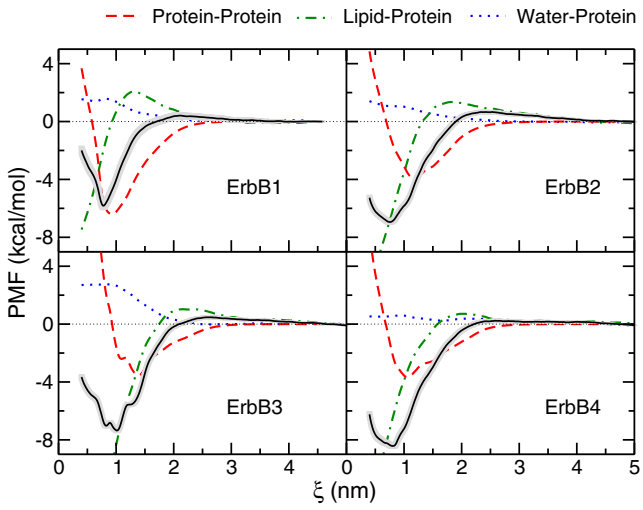

FIGURE 3 PMF as a function of lateral separation with decomposition to major contributions. The shaded area is an estimate of the error extracted as described in the text.

water-induced contributions are repulsive due to the removal of favorable interactions of hydrophilic residues with water. Clearly, such contributions depend on the ability of the model to capture water-water and water-protein interactions. It should be noted that CG water models generally present several limitations for studies attempting to simultaneously match different thermodynamic properties or predict phase diagrams, and improvements are actively being sought (58,59). The magnitude of water-induced interactions, as probed in our study, is not negligible and depends on both the extent of the domain in the aqueous phase and the chemistry of the interfacial amino acids. In this study, domains were modeled with 27 residues, and less tilting implies an increase of solvent-protein contacts; this effect is increased for ErbB3 due to larger interfacial residues. We also note that previous experiments suggested the existence of a negative regulatory influence from the extramembranous portions that inhibit dimerization under certain conditions (18,31,60). A recent study with FGFR3 TM domains reported that the removal of juxtamembrane residues induced dimerization comparable to that observed with GpA (61), which was attributed to potential steric hindrance between these residues.

Protein-protein and lipid-mediated contributions

To gain further insight, we directly compared protein-protein and lipid-mediated interactions among the four systems studied. Due to the increased complexity introduced by differences in sequences, we resorted to additional calculations to interpret our results. Fig. 4 presents free-energy data for the TM domains side-by-side with measures of SASA and SEV in the hydrophobic regime for each pair as a function of ξ. Fig. 5 presents selected configurations and the average tilt τ angle of the proteins as a function of ξ.

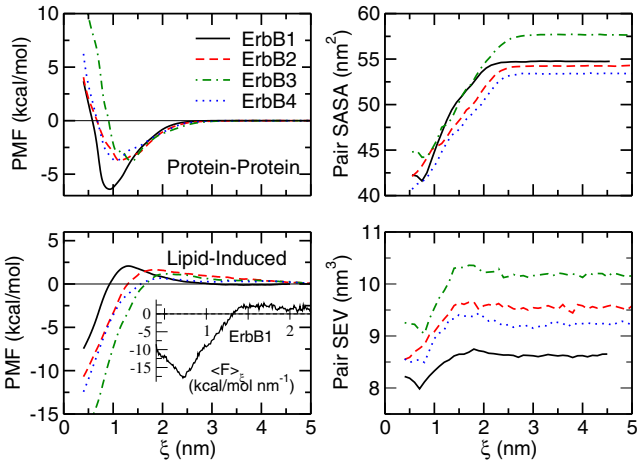

FIGURE 4 PMF decomposition into protein-protein and lipid-mediated along with the SASA and SEV. Volume was calculated only inside the hydrophobic domain as described in text. The inset at the bottom left presents the lipid-induced $< F >_\xi$ on the ErbB1 pair below 2.25 nm.

First, we examine protein-protein interactions, which are important at intermediate distances and compete with lipid-mediated repulsion. The most extended favorable contributions are present for the ErbB1 pair due to low tilting of this domain in the membrane environment. The larger volume of ErbB3 leads to repulsive interactions at low distances, thereby preventing the proteins from approaching further. Protein-protein interactions are commonly characterized by the area of the interface formed (11,62,63). The SASA for each pair of proteins is provided in Fig. 5 (*top right*) as a function of ξ. The decrease between large separations and dimer state signifies the formation of a buried area between the TM domains that is not accessible to the solvent. This area (at the minimum of the PMF $\xi \approx 0.8$, except for ErbB3, where $\xi \approx 1.0$ nm) is presented in Table 1. Similar values (≈ 8 nm^2)

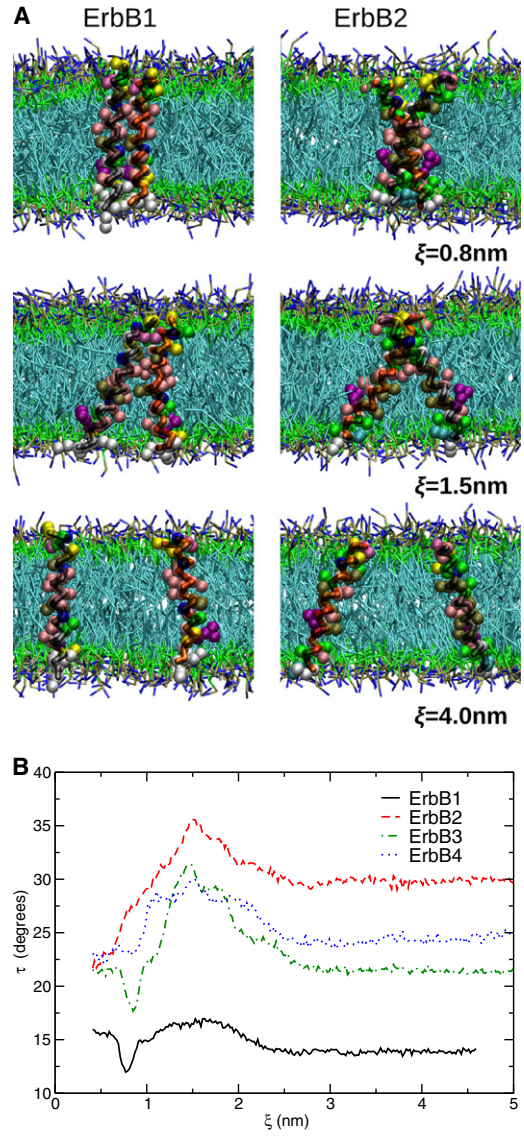

FIGURE 5 (*A*) Selected configurations of ErbB1 and ErbB2 pairs at different separations (water not shown, for clarity). (*B*) Average tilt angle (τ) as a function of separation.

were obtained in a previous study with shorter dimers of GpA (63). It is noteworthy that ErbB2 and ErbB4 continuously increase the dimer interface area below 1 nm, which is not the case for the other two members of the family. Furthermore, although some agreement is found, the surface areas of the interface do not necessarily match the magnitude of the minima in protein-protein interactions. There are two possible explanations for this: 1), the area does not account for the strength of the interaction between specific amino acids; and 2), the minima do not coincide with the total PMF minima. As the proteins approach closer, the interfacial area increases, but the actual interactions may be repulsive due to steric hindrances. For ErbB3 the minimum in protein-protein interactions is located at ≈ 1.5 nm; nevertheless, the proteins reduce their separation due to favorable membrane-mediated attraction.

Lipid-mediated interactions present two regimes: at long distances, removal of lipid molecules is unfavorable, leading to a repulsive contribution. The magnitude of this repulsion is the result of lipid-protein enthalpic interactions that do not scale monotonically with protein tilting, as previously observed for GpA in lipid bilayers (24). ErbB2, despite higher tilting, displays stronger repulsions compared to ErbB4. However, the differences are relatively small compared to our findings on lipid-induced attraction experienced at short separations. The range of magnitude of these contributions differs significantly among the four domains. To interpret this result, it is necessary to recall that depletion forces between two bodies in a fluid medium are proportional to the overlap between the SEVs (4,64). To define quantitatively the solvent-excluded volume, the use of a probe of 0.14 nm is inappropriate because the volume of a lipid is higher (65). However, only lipid tails located in the hydrophobic regime of the bilayer are expected to contribute to such a depletion attraction. Even in this regime, significant heterogeneity in lipid tail entropy is expected (66). Furthermore, in the model used here, the lipid CG bead has a 0.235 nm radius. We maintained the same probe radius (0.14 nm) for our analysis; however, we emphasize the qualitative character of the data. In addition, we found it necessary (due to tilting effects) to restrict calculations to the portions of protein molecules that were within the hydrophobic regime of the bilayer. Protein volume calculations were performed only for the beads of each helix located between the average position of DPPC glycerol beads in each leaflet (in contrast to Table 1, for which all beads were used).

Fig. 4 reveals several intriguing features. The order of the solvent-excluded volumes matches the favorable induced depletion attraction. Decreasing helical separation is a mechanism to increase entropy of the system by increasing the available volume to lipid tails; however, at intermediate distances, a small increase is observed. This finding suggests that the previously discussed repulsive peak in lipid-induced interactions is not solely enthalpic but also incorporates an unfavorable decrease of lipid entropy. The latter is induced by increased protein tilting at these distances (Fig. 5). At short separations, lipids are depleted in-between proteins and the lipid-accessible volume increases as helices approach further at values of ξ where the lipid-induced free energy is ≈ 0. Our analysis, though, suggests that lipid entropy is not increased only by a decrease in protein separation. A clear minimum of the volume of the ErbB1 pair is coupled with an abrupt decrease of tilt angle τ (Fig. 5). Decreasing τ is an additional mechanism to benefit from an increase in lipid-accessible volume and occurs simultaneously as proteins approach the overall PMF minimum. A parallel arrangement of the helices does not facilitate the packing along specific motifs, as proposed by Russ and Engelman (8), even if they are present in the amino-acid sequence. ErbB2 and ErbB4 are able to form these close-packed structures. However, this is not the case for ErbB1, due to the unfavorable increase in tilting required. This effect is not a result of solely enthalpic contributions; the volume of the pair will increase, leading to higher lipid-induced forces. This is further demonstrated by plotting the lipid-induced force for ErbB1 in the inset of Fig. 5 (*lower left*). A similar transition was observed for GpA in DPPC (24), although the balance of the forces present was such that a shift to higher τ-values and a sequence-specific dimer was favored.

Dimer characterization

To complete our view of association of these TM domains and further support our findings, we characterized the configurations sampled. We employed three measures, all calculated as a function of ξ: the average tilt angle τ (Fig. 5), the crossing angle Ω, and the interfaces formed using the residue distance maps. Selected data are presented in Fig. 6 and should be examined in comparison with Fig. 3, which provides the probability of observing a certain separation ξ. For consistency, we probed the interfaces sampled (Fig. 6, *C* and *D*) within a thermally accessible k_BT range of ξ around the minimum of the total PMF. Note that this results in a significantly larger span for ErbB2. Despite the increased range of ξ, ErbB2 appears to form sequence-specific dimers, in contrast to ErbB1, which presents a parallel arrangement with crossing angles $\Omega \approx -20$ to $+20$ (Fig. 6 *A*). For decreased separations between ErbB1 helices, the dimer moves to a right-handed packing; however, this is not favored by the free-energy profile in Fig. 3. For ErbB3 (despite the parallel arrangement) and ErbB4, a preference was found to form interfaces with the smaller residues, given that this will maximize the overlap of the SEV. An interesting feature observed is that the TM domains of ErbB2 appear to contribute to the formation of a dimer with contacts closer to the C-terminus, as shown in Fig. 6 *D*. It is noteworthy that with regard to the full receptor, this configuration is proposed to correspond to a nonactivated state (67,68), which supports the notion that preformed dimers do not necessarily correspond to activated receptors. Finally, we note that

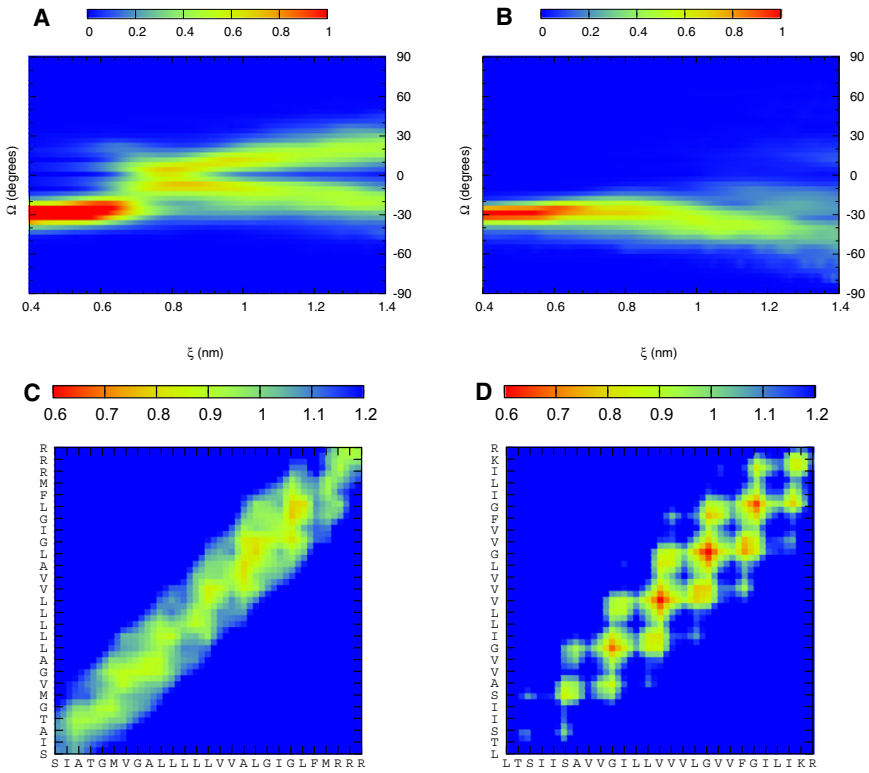

FIGURE 6 (*A* and *B*) Crossing angle Ω for (*A*) ErbB1 and (*B*) ErbB2. (*C* and *D*) Average interface at ξ-values within k_BT of the PMF minimum for (*C*) ErbB1 ($0.71 < \xi < 0.81$ nm) and (*D*) ErbB2 ($0.46 < \xi < 0.91$ nm).

a previous study using ^{2}H NMR spectroscopy reported rotational modes with a higher frequency for ErbB1 compared to ErbB2 (18), indicating that ErbB1 appeared primarily in the monomeric state, in contrast to ErbB2, which was found mostly in the dimer state. Our results are not necessarily in disagreement: a parallel nonspecific arrangement of ErbB1 pairs would allow a considerable degree of rotational modes to be present, in contrast to the close specific packing of ErbB2, which restricts such individual protein motion.

Comparison with experiments

Several studies have examined the association affinity of ErbB TM domains using experimental techniques. Given the complexity of the factors controlling the association process, and the differences in the methods involved, it is not surprising to find that a quantitative comparison is not straightforward. Our free-energy profiles as a function of lateral separation can be integrated along cylindrical coordinates to obtain the association constant (24). The standard free energies per 1 M of hydrophobic phase were calculated as -6.10 ± 0.15, -7.64 ± 0.16, -8.03 ± 0.15, -9.10 ± 0.17 kcal/mol, and can be compared with our previous findings of -7.9 ± 0.2 kcal/mol for GpA (24). Thus our predictions support the notion that TM domains of ErbB4 present a stronger affinity to form dimers than GpA in DPPC bilayers, in contrast to other members of the family.

Recent fluorescence resonance energy transfer experiments reported a value of -2.5 kcal/mol for ErbB1 in DLPC (41), a value significantly higher than our result. This is expected in part due to the environment (DPPC herein (24)) and potential inhibition between the donor and acceptor sequences added. We also add that three-body contributions (not accounted for in our study) would reduce the affinity of proteins to dimerize (69). It would be interesting to compare data extracted from all four TM domains using such measurements.

Several other experimental studies reported data for all members (36,39,40,42); unfortunately, association was probed indirectly by a signaling mechanism involving chimera proteins in complex hydrophobic environments. The nature of the environment is a significant factor, as shown by recent measurements of GpA association in mammalian cell membranes (70). The association affinity is often reported in a qualitative scheme comparing to GpA. Fluorescence resonance energy transfer experiments in detergents revealed strong interactions for the first three members with a relative rank of GpA > ErbB2 > ErbB1 > ErbB3 > ErbB4 (42,71). Recent TOXCAT measurements reported self-interactions for a number of TM domains; for our systems, the propensities were ErbB2 > GpA > ErbB1 > ErbB4 ≈ ErbB3 (40). Earlier TOXCAT experiments also supported the self-association of these sequences in the following order: GpA > ErbB4 > ErbB1 ≈ ErbB2 > ErbB3 (36), and another set of measurements with the TOXCAT system resulted in GpA > ErbB1> ErbB2 (39). Qualitatively, both the experimental data and our simulations support a significant affinity to self-associate; however, there is no quantitative agreement between the studies, and thus there is a clear need for further research to

probe such thermodynamics. We note that the actual values appear more consistent for ErbB1, which presents the least tilting flexibility (Fig. 1) and potentially is less susceptible to changes in different hydrophobic environments. Our study is the only one in which ErbB4 was found to be the strongest pair. The high tilting flexibility of this sequence, together with potential stronger repulsive interactions by extramembrane domains, could contribute to this discrepancy.

CONCLUSIONS

We performed parallel Monte Carlo simulations to quantify the self-association affinity of the TM domains of ErbBs in a lipid bilayer. Extensive analyses with different amino-acid sequences allowed us to gain further insight into the factors controlling helix association. Specifically, we found that recognition is initiated by favorable protein-protein interactions. Their extent is dependent on the ability of helices to tilt, and is opposed by lipid-protein enthalpic and entropic contributions. When all lipid molecules between the helices are excluded, depletion attraction and direct interactions are the major forces driving dimerization. However, decreasing separation is not the sole mechanism for increasing lipid entropy, since a more parallel arrangement is favored by lipid molecules. It is evident that proteins approach at separations shorter than the minimum of protein-protein interactions. At such proximity, the ability to increase lipid entropy is sequence-specific; decreasing interhelical separation is a mechanism that depends on the presence of small residues. Another additional contribution arises from the ability of helices to align parallel to the membrane normal. Our results are in agreement with experiments suggesting that residues distant from the interface modulate dimerization affinity (13), and recent simulations using an implicit membrane model that have shown the critical role of interfacial residues (14). In this study we performed a quantitative assessment of changes in membrane-mediated interactions, and we note that the latter are expected to be highly dependent on environmental specifics (24).

Finally, our work highlights the complex character of helix association in membranes and the need for further quantitative experimental and simulation studies. Simulations are needed to account for protein concentration effects, examine association in a multicomponent membrane environment, and improve the resolution of the models considered. A viable approach for increasing resolution was described in recent studies that focused on reconstructing AT detail using sampled CG configurations (72,73); however, such an approach was beyond the scope of this study.

We thank the University of Houston Research Computing Center for the generous allocation of CPU time on the Maxwell cluster. Computations on IBM's Power7 high-performance cluster (BlueBioU) were supported by a 2010 IBM Shared University Research Award to Rice University as part of IBM's Smarter Planet Initiatives in Life Science/Healthcare and in collaboration with the Texas Medical Center, with additional contributions from IBM, CISCO, Qlogic, and Adaptive Computing.

Financial support for this work was provided by the University of Houston (GEAR IO96691).

REFERENCES

1. Lee, A. G. 2004. How lipids affect the activities of integral membrane proteins. *Biochim. Biophys. Acta.* 1666:62–87.
2. Lee, A. G. 2003. Lipid-protein interactions in biological membranes: a structural perspective. *Biochim. Biophys. Acta.* 1612:1–40.
3. Mackenzie, K. R. 2006. Folding and stability of α-helical integral membrane proteins. *Chem. Rev.* 106:1931–1977.
4. Sintes, T., and A. Baumgärtner. 1997. Protein attraction in membranes induced by lipid fluctuations. *Biophys. J.* 73:2251–2259.
5. Lagüe, P., M. J. Zuckermann, and B. Roux. 2000. Lipid-mediated interactions between intrinsic membrane proteins: a theoretical study based on integral equations. *Biophys. J.* 79:2867–2879.
6. Lagüe, P., M. J. Zuckermann, and B. Roux. 2001. Lipid-mediated interactions between intrinsic membrane proteins: dependence on protein size and lipid composition. *Biophys. J.* 81:276–284.
7. de Meyer, F. J.-M., M. Venturoli, and B. Smit. 2008. Molecular simulations of lipid-mediated protein-protein interactions. *Biophys. J.* 95:1851–1865.
8. Russ, W. P., and D. M. Engelman. 2000. The GxxxG motif: a framework for transmembrane helix-helix association. *J. Mol. Biol.* 296:911–919.
9. Lemmon, M. A., J. M. Flanagan, …, D. M. Engelman. 1992. Glycophorin A dimerization is driven by specific interactions between transmembrane α-helices. *J. Biol. Chem.* 267:7683–7689.
10. Lemmon, M. A., H. R. Treutlein, …, D. M. Engelman. 1994. A dimerization motif for transmembrane α-helices. *Nat. Struct. Biol.* 1: 157–163.
11. MacKenzie, K. R., J. H. Prestegard, and D. M. Engelman. 1997. A transmembrane helix dimer: structure and implications. *Science.* 276:131–133.
12. Brosig, B., and D. Langosch. 1998. The dimerization motif of the glycophorin A transmembrane segment in membranes: importance of glycine residues. *Protein Sci.* 7:1052–1056.
13. Doura, A. K., and K. G. Fleming. 2004. Complex interactions at the helix-helix interface stabilize the glycophorin A transmembrane dimer. *J. Mol. Biol.* 343:1487–1497.
14. Zhang, J., and T. Lazaridis. 2009. Transmembrane helix association affinity can be modulated by flanking and noninterfacial residues. *Biophys. J.* 96:4418–4427.
15. Johnson, R. M., A. Rath, …, C. M. Deber. 2006. Lipid solvation effects contribute to the affinity of Gly-xxx-Gly motif-mediated helix-helix interactions. *Biochemistry.* 45:8507–8515.
16. Zhang, J., and T. Lazaridis. 2006. Calculating the free energy of association of transmembrane helices. *Biophys. J.* 91:1710–1723.
17. Ozdirekcan, S., C. Etchebest, …, P. F. Fuchs. 2007. On the orientation of a designed transmembrane peptide: toward the right tilt angle? *J. Am. Chem. Soc.* 129:15174–15181.
18. Sharpe, S., K. R. Barber, and C. W. M. Grant. 2002. Evidence of a tendency to self-association of the transmembrane domain of ErbB-2 in fluid phospholipid bilayers. *Biochemistry.* 41:2341–2352.
19. Rigby, A. C., K. R. Barber, …, C. W. Grant. 1996. Transmembrane region of the epidermal growth factor receptor: behavior and interactions via ^{2}H NMR. *Biochemistry.* 35:12591–12601.
20. Monticelli, L., S. K. Kandasamy, …, S.-J. Marrink. 2008. The MARTINI coarse-grained force field: extension to proteins. *J. Chem. Theory Comput.* 4:819–834.
21. Bond, P. J., and M. S. P. Sansom. 2006. Insertion and assembly of membrane proteins via simulation. *J. Am. Chem. Soc.* 128:2697–2704.

22. Psachoulia, E., P. W. Fowler, …, M. S. Sansom. 2008. Helix-helix interactions in membrane proteins: coarse-grained simulations of glycophorin a helix dimerization. *Biochemistry.* 47:10503–10512.

23. Janosi, L., and M. Doxastakis. 2009. Accelerating flat-histogram methods for potential of mean force calculations. *J. Chem. Phys.* 131:054105.

24. Janosi, L., A. Prakash, and M. Doxastakis. 2010. Lipid-modulated sequence-specific association of glycophorin A in membranes. *Biophys. J.* 99:284–292.

25. Bublil, E. M., and Y. Yarden. 2007. The EGF receptor family: spearheading a merger of signaling and therapeutics. *Curr. Opin. Cell Biol.* 19:124–134.

26. Schlessinger, J. 2000. Cell signaling by receptor tyrosine kinases. *Cell.* 103:211–225.

27. Hynes, N. E., and H. A. Lane. 2005. ERBB receptors and cancer: the complexity of targeted inhibitors. *Nat. Rev. Cancer.* 5:341–354.

28. Tao, R.-H., and I. N. Maruyama. 2008. All EGF(ErbB) receptors have preformed homo- and heterodimeric structures in living cells. *J. Cell Sci.* 121:3207–3217.

29. Landau, M., and N. Ben-Tal. 2008. Dynamic equilibrium between multiple active and inactive conformations explains regulation and oncogenic mutations in ErbB receptors. *Biochim. Biophys. Acta.* 1785:12–31.

30. Moore, D. T., B. W. Berger, and W. F. DeGrado. 2008. Protein-protein interactions in the membrane: sequence, structural, and biological motifs. *Structure.* 16:991–1001.

31. Tanner, K. G., and J. Kyte. 1999. Dimerization of the extracellular domain of the receptor for epidermal growth factor containing the membrane-spanning segment in response to treatment with epidermal growth factor. *J. Biol. Chem.* 274:35985–35990.

32. Bargmann, C. I., and R. A. Weinberg. 1988. Oncogenic activation of the neu-encoded receptor protein by point mutation and deletion. *EMBO J.* 7:2043–2052.

33. Tzahar, E., R. Pinkas-Kramarski, …, Y. Yarden. 1997. Bivalence of EGF-like ligands drives the ErbB signaling network. *EMBO J.* 16:4938–4950.

34. Brennan, P. J., T. Kumagai, …, T. Kumogai. 2000. HER2/neu: mechanisms of dimerization/oligomerization. *Oncogene.* 19:6093–6101.

35. Li, E., and K. Hristova. 2006. Role of receptor tyrosine kinase transmembrane domains in cell signaling and human pathologies. *Biochemistry.* 45:6241–6251.

36. Mendrola, J. M., M. B. Berger, …, M. A. Lemmon. 2002. The single transmembrane domains of ErbB receptors self-associate in cell membranes. *J. Biol. Chem.* 277:4704–4712.

37. Bennasroune, A., M. Fickova, …, P. Hubert. 2004. Transmembrane peptides as inhibitors of ErbB receptor signaling. *Mol. Biol. Cell.* 15:3464–3474.

38. Bennasroune, A., A. Gardin, …, P. Hubert. 2004. Tyrosine kinase receptors as attractive targets of cancer therapy. *Crit. Rev. Oncol. Hematol.* 50:23–38.

39. Bennasroune, A., A. Gardin, …, P. Hubert. 2005. Inhibition by transmembrane peptides of chimeric insulin receptors. *Cell. Mol. Life Sci.* 62:2124–2131.

40. Finger, C., C. Escher, and D. Schneider. 2009. The single transmembrane domains of human receptor tyrosine kinases encode self-interactions. *Sci. Signal.* 2:ra56.

41. Chen, L., M. Merzlyakov, …, K. Hristova. 2009. Energetics of ErbB1 transmembrane domain dimerization in lipid bilayers. *Biophys. J.* 96:4622–4630.

42. Duneau, J.-P., A. P. Vegh, and J. N. Sturgis. 2007. A dimerization hierarchy in the transmembrane domains of the HER receptor family. *Biochemistry.* 46:2010–2019.

43. van Gunsteren, W. F., S. R. Billeter, …, I. G. Tironi. 1996. Biomolecular simulation: the GROMOS96 manual and user guide. Vdf Hochschulverlag AG an der ETH Zurich, Zurich.

44. Oostenbrink, C., A. Villa, …, W. F. van Gunsteren. 2004. A biomolecular force field based on the free enthalpy of hydration and solvation: the GROMOS force-field parameter sets 53A5 and 53A6. *J. Comput. Chem.* 25:1656–1676.

45. Van Der Spoel, D., E. Lindahl, …, H. J. Berendsen. 2005. GROMACS: fast, flexible, and free. *J. Comput. Chem.* 26:1701–1718.

46. Lee, J., and W. Im. 2008. Transmembrane helix tilting: insights from calculating the potential of mean force. *Phys. Rev. Lett.* 100:018103.

47. Jones, D. H., K. R. Barber, …, C. W. Grant. 1998. Epidermal growth factor receptor transmembrane domain: ^{2}H NMR implications for orientation and motion in a bilayer environment. *Biochemistry.* 37:16780–16787.

48. Eisenhaber, F., P. Lijnzaad, …, M. Scharf. 1995. The double cubic lattice method–efficient approaches to numerical integration of surface area and volume and to dot surface contouring of molecular assemblies. *J. Comput. Chem.* 16:273–284.

49. Connoly, M. L. 1985. Computation of molecular volume. *J. Am. Chem. Soc.* 107:1118–1124.

50. Rees, D. C., and G. M. Wolfe. 1993. Macromolecular solvation energies derived from small molecule crystal morphology. *Protein Sci.* 2:1882–1889.

51. Wang, F. G., and D. P. Landau. 2001. Efficient, multiple-range random walk algorithm to calculate the density of states. *Phys. Rev. Lett.* 86:2050–2053.

52. Kim, E. B., R. Faller, …, J. J. de Pablo. 2002. Potential of mean force between a spherical particle suspended in a nematic liquid crystal and a substrate. *J. Chem. Phys.* 117:7781–7787.

53. Doxastakis, M., Y.-L. Chen, and J. J. de Pablo. 2005. Potential of mean force between two nanometer-scale particles in a polymer solution. *J. Chem. Phys.* 123:34901.

54. Sengupta, D., and S. J. Marrink. 2010. Lipid-mediated interactions tune the association of glycophorin A helix and its disruptive mutants in membranes. *Phys. Chem. Chem. Phys.* 12:12987–12996.

55. Marsh, D. 2008. Protein modulation of lipids, and vice-versa, in membranes. *Biochim. Biophys. Acta.* 1778:1545–1575.

56. Allen, M. P., and D. J. Tildesley. 1987. Computer Simulation of Liquids. Oxford University Press, New York.

57. Press, W. H., S. A. Teukolsky, …, B. P. Flannery. 2007. Numerical Recipes: The Art of Scientific Computing, 3rd ed. Cambridge University Press, New York.

58. He, X., W. Shinoda, …, M. L. Klein. 2010. Exploring the utility of coarse-grained water models for computational studies of interfacial systems. *Mol. Phys.* 108:2007–2020.

59. Yesylevskyy, S. O., L. V. Schäfer, …, S. J. Marrink. 2010. Polarizable water model for the coarse-grained MARTINI force field. *PLOS Comput. Biol.* 6:e1000810.

60. Ferguson, K. M., M. B. Berger, …, M. A. Lemmon. 2003. EGF activates its receptor by removing interactions that autoinhibit ectodomain dimerization. *Mol. Cell.* 11:507–517.

61. Peng, W. C., X. Lin, and J. Torres. 2009. The strong dimerization of the transmembrane domain of the fibroblast growth factor receptor (FGFR) is modulated by C-terminal juxtamembrane residues. *Protein Sci.* 18:450–459.

62. Fleming, K. G., A. L. Ackerman, and D. M. Engelman. 1997. The effect of point mutations on the free energy of transmembrane α-helix dimerization. *J. Mol. Biol.* 272:266–275.

63. Hénin, J., A. Pohorille, and C. Chipot. 2005. Insights into the recognition and association of transmembrane α-helices. The free energy of α-helix dimerization in glycophorin A. *J. Am. Chem. Soc.* 127: 8478–8484.

64. Asakura, S., and F. Oosawa. 1954. On interaction between two bodies immersed in a solution of macromolecules. *J. Chem. Phys.* 22: 1255–1256.

65. Armen, R. S., O. D. Uitto, and S. E. Feller. 1998. Phospholipid component volumes: determination and application to bilayer structure calculations. *Biophys. J.* 75:734–744.

66. Doxastakis, M., V. G. Sakai, …, J. J. de Pablo. 2007. A molecular view of melting in anhydrous phospholipidic membranes. *Biophys. J.* 92:147–161.

67. Fleishman, S. J., J. Schlessinger, and N. Ben-Tal. 2002. A putative molecular-activation switch in the transmembrane domain of erbB2. *Proc. Natl. Acad. Sci. USA*. 99:15937–15940.

68. Bocharov, E. V., K. S. Mineev, …, A. S. Arseniev. 2008. Spatial structure of the dimeric transmembrane domain of the growth factor receptor ErbB2 presumably corresponding to the receptor active state. *J. Biol. Chem.* 283:6950–6956.

69. Yiannourakou, M., L. Marsella, …, B. Smit. 2010. Towards an understanding of membrane-mediated protein-protein interactions. *Faraday Discuss.* 144:359–367, discussion 445–481.

70. Chen, L., L. Novicky, …, K. Hristova. 2010. Measuring the energetics of membrane protein dimerization in mammalian membranes. *J. Am. Chem. Soc.* 132:3628–3635.

71. Fisher, L. E., D. M. Engelman, and J. N. Sturgis. 1999. Detergents modulate dimerization, but not helicity, of the glycophorin A transmembrane domain. *J. Mol. Biol.* 293:639–651.

72. Rzepiela, A. J., L. V. Schäfer, …, S. J. Marrink. 2010. Reconstruction of atomistic details from coarse-grained structures. *J. Comput. Chem.* 31:1333–1343.

73. Psachoulia, E., D. P. Marshall, and M. S. P. Sansom. 2010. Molecular dynamics simulations of the dimerization of transmembrane α-helices. *Acc. Chem. Res.* 43:388–396.